Materials Science Forum
ISSN: 1662-9752, Vol. 1184, pp 113-121
doi:10.4028/p-3JRLbf

Submitted: 2026-01-24
Accepted: 2026-02-23
Online: 2026-04-14

Towards Multi-Scale Friction Modelling for Bulk Sheet Metal Forming Applications

Aratz Barandiaran[1,a], Alaitz Zabala[1,b], David Abedul[1,c], Javad Hazrati[2,d] and Lander Galdos[1,e*]

[1]Material and industrial production department, Mondragon University, Loramendi 4, 20500 Arrasate-Mondragon, Spain

[2]Nonlinear Solid Mechanics, Faculty of Engineering Technology, University of Twente, Enschede, Netherlands

[a]aratz.barandiaran@alumni.mondragon.edu, [b]azabalae@mondragon.edu, [c]dabedul@mondragon.edu, [d]j.hazratimarangalou@utwente.nl, [e]lgaldos@mondragon.edu (*corresponding author)

Keywords: Sheet metal forming, tribology, friction modelling

Abstract. Cold forging and sheet-metal bulk forming operations typically involve severe deformation, high contact pressures, and substantial surface enlargement. As highlighted in previous studies, friction behavior under these extreme conditions is governed by temperature, contact pressure, sliding velocity, and changes in the real contact area due to surface expansion.
This work presents a newly developed linear sliding tribotester designed to characterize the friction response of metal sheets subjected to sheet-metal bulk forming conditions. The testing procedure consists of two stages. In the first stage, the sample is compressed to intentionally modify and enlarge the initial contact surface, with the degree of surface expansion controlled by the specimen geometry. In the second stage, once the surface has been altered, frictional contact is generated between the sample and a sliding table, enabling the measurement of normal and tangential forces. These force measurements are subsequently used to determine the mean coefficient of friction.
The results obtained constitute the first dataset toward the development of a multi-scale friction model for sheet-metal bulk gear forging. This model aims to incorporate the effects of extreme contact pressures, asperity flattening, and lubricant-related hydrostatic and hydrodynamic mechanisms.

Introduction

Computer-aided process optimization is widely implemented in the cold forging sector, where finite element (FE) simulations are routinely employed to predict die filling, identify defects such as folds, and estimate forming loads. These tools make it possible to design multi-stage forging sequences efficiently and with reduced development time. Nonetheless, the fidelity of numerical predictions strongly depends on the quality of the input definitions. Key parameters - including constitutive material data and friction coefficients - as well as numerical aspects such as mesh refinement, element selection, and the applied solution schemes, significantly influence the robustness of the results.

Historically, FE simulations for cold forging have relied on isotropic hardening laws combined with isotropic yield criteria and associated flow rules. Recent research has examined the impact of load path reversals, strain-rate sensitivity, and adiabatic temperature increase on the accuracy of numerical simulations. The introduction of kinematic hardening models has revealed notable effects on residual stresses and forming forces, especially in processes where the material undergoes flow reversal, such as forward extrusion followed by compression [11, 2, 3]. Moreover, the influence of strain rate and adiabatic heating on the overall material behavior in such simulations has been demonstrated in recent works [4].

Regarding friction modeling, most cold forging simulations still use constant friction coefficients. However, knowledge from the stamping field shows that friction is highly dependent on the specific contact conditions. Variable friction formulations have been proposed based on micro-scale

investigations [8, 10] as well as macro-scale tribological studies [1, 17, 18] for sheet metal stamping. There is broad consensus that friction is influenced primarily by contact pressure and sliding velocity [13]. Higher pressures tend to flatten surface asperities, modifying the contact geometry and subsequently the friction response [12]. Likewise, increasing sliding velocity typically contributes to a reduction in friction due to improved lubrication conditions. Friction laws depending on both pressure and velocity have therefore become increasingly common in sheet-metal forming simulations, supported by commercial software solutions such as Triboform. Industrial applications have shown clear improvements in prediction accuracy when these advanced models are applied [5, 15, 9, 16].

In cold forging operations, frictional behavior becomes even more complex because the processes involve extreme contact pressures, pronounced sliding, and considerable surface enlargement, all of which drastically modify interface conditions. Numerous tribometers have been developed to study these effects. The friction subgroup of the International Cold Forging Group provided an extensive review of existing tribotesters in [7], noting that many devices exhibit limited or fixed ranges of operation. To extend these capabilities, Groche et al. proposed the Sliding Compression Test (SCT), in which cylindrical specimens are first compressed with different anvil geometries to generate controlled surface expansion and are thereafter translated against a flat counterface under predefined pressures [6]. Similarly, aiming to reach higher surface enlargement and assess solid lubricant performance for cold forging, Wang et al. introduced a multi-stage forging test involving an upsetting operation followed by ironing with three metallic balls, enabling detailed investigation of lubricant behavior and adhesion phenomena [19].

This study introduces the Sheet Sliding Compression Test (SSCT), a novel tribological method developed to analyze lubricant performance under conditions that combine elevated contact pressures with significant surface expansion. Owing to its wide operational window, the SSCT is suitable for characterizing lubricants used both in cold forging and sheet-bulk metal forming processes. The apparatus integrates load sensors that continuously record normal and tangential forces during sliding, enabling direct determination of the mean coefficient of friction throughout the experiment. The SSCT methodology is validated using commercially pure aluminum sheets tested under different levels of contact pressure and surface expansion, aiming to develop a multi-scale friction model for sheet bulk metal forming in the near future.

The Sheet Sliding Compression Test (SSCT)

Test description. The operating principle of the SSCT is depicted in Fig. 1. As shown, the procedure consists of two clearly differentiated stages. In the first stage, the specimen is vertically compressed against a flat counter-tool, generating a normal load and causing an enlargement of the contact area. The extent of this surface expansion is determined by the specimen geometry, which will be discussed later. Once the required surface enlargement and contact pressure have been achieved, the flat tool is displaced relative to the specimen. This motion enables the measurement of both normal and tangential forces, from which the mean coefficient of friction is obtained. During this second stage, the contact pressure may be kept equal to that used during the compression phase or reduced to lower values in order to examine the frictional response of the newly formed surface under different loading conditions.

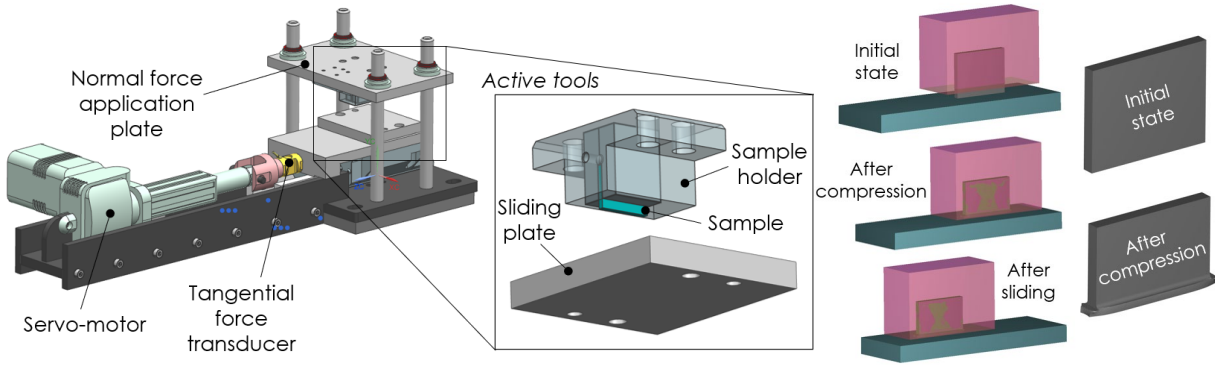

Fig.1. Principle of the new Sheet Compression Sliding Test (SCTT). Tool design with relevant features and different test stages

Test samples can be manufactured by wire EDM, either starting from cylindrical bars for cold forging studies or from thick sheets for applications related to bulk sheet metal forming. The surface finish of the samples can be tailored through different machining or finishing processes. As presented in the next sections, in this investigation the surface roughness was effectively controlled by the wire EDM process. However, alternative surface conditions - such as those produced by milling, grinding or shearing - can also be evaluated using the new testing device. Likewise, the sliding plate, which represents the forming tool in real processes, is a flat interchangeable element that can be replaced to analyze different materials or surface textures.

The sliding velocity is controlled through a servo-motor system, allowing the test to cover a wide range of kinematic conditions. The main purpose of the new tribotester is to support the development of multi-scale friction models that incorporate the influence of contact pressure, sliding speed, and the evolution or flattening of surface roughness. To construct such models, comprehensive experimental datasets obtained with this device are required for accurate calibration.

Friction coefficient evaluation method. Fig. 2 presents an example of the force signals obtained during one of the tribological tests, clearly illustrating the two distinct steps of the test. In the first step, the compression phase, the sample holder moves downward, causing the normal force to increase until it reaches a predefined value. Once this value is achieved, the vertical movement is stopped to allow the normal force to stabilize before the sliding phase begins. During the sliding phase, the sample holder remains stationary while the servomotor is activated to move the sliding plate at a constant velocity. Throughout this phase, both the friction force and the normal force are measured. As shown in the figure, both forces are displacement-dependent, consistent with observations reported in [6].

The friction coefficient can be calculated during the sliding phase as the ratio between the tangential force and the normal force, and it varies over time. To facilitate the comparison of different tribological conditions, the mean friction coefficient is calculated as the average value of the friction coefficient within a defined evaluation area, using Eq. 1:

$$\bar{\mu} = {\sum_{i=1}^{n} \mu_i}/{n} \tag{1}$$

where $\bar{\mu}$ is the mean friction coefficient, μ_i is the instantaneous friction value and n is the total amount of friction coefficients measured in the evaluation area, which is selected by removing the acceleration and breaking instants of the servomotor (see Fig. 2 right).

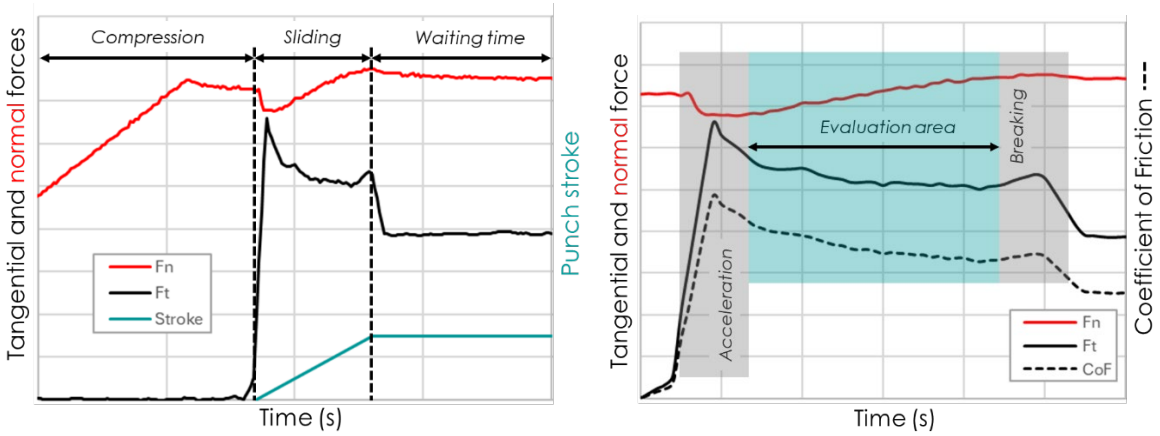

Fig. 2. Different steps of the SCST together with the measured force signals and definition of the evaluation area to calculate the mean friction value.

Experimental Methodology

Tested material and samples dimensions. The experimental campaign was carried out using AA1050 aluminum sheets with a nominal thickness of 3 mm. The flow behavior of the material at room temperature was characterized through uniaxial tensile tests conducted on an Instron universal testing machine. The apparatus was equipped with a ZwickRoell makroXtens II contact extensometer, and all tests were performed in accordance with the ASTM E08 standard. The material exhibited very limited strain hardening and reached its saturation flow stress rapidly. This response can be accurately described using the Voce hardening law (Eq. 2), expressed as:

$$\sigma = 117.7 \cdot \left[1 - 0.1475 \cdot e^{\left(-1238.9 \cdot \varepsilon_p\right)}\right] \quad (2)$$

Two different specimen geometries were employed in the present investigation. The first configuration consisted of a small sample with a contact surface of 5 × 3 mm², designed to assess contact conditions involving high normal pressures without inducing surface expansion (see Fig. 3 left). The 5 mm contact length ensured a uniform pressure distribution, avoiding the non-uniform contact stresses typically observed in specimens with a 30 mm length. To suppress any possibility of surface enlargement during compression, the free distance between the specimen holder and the sliding plate was restricted to 0.5 mm.

The second configuration consisted of a larger specimen with an initial contact area of 30 × 3 mm², intended to reproduce conditions in which significant surface expansion occurs. To prevent buckling or cracking of the material near the clamping region, the tool edges were rounded using a 1 mm radius fillet. In this setup, additional material was necessary to accommodate the expected expansion of the contact area; therefore, a free length of 5 mm was maintained between the sample holder and the sliding plate, as illustrated in Fig. 3 right.

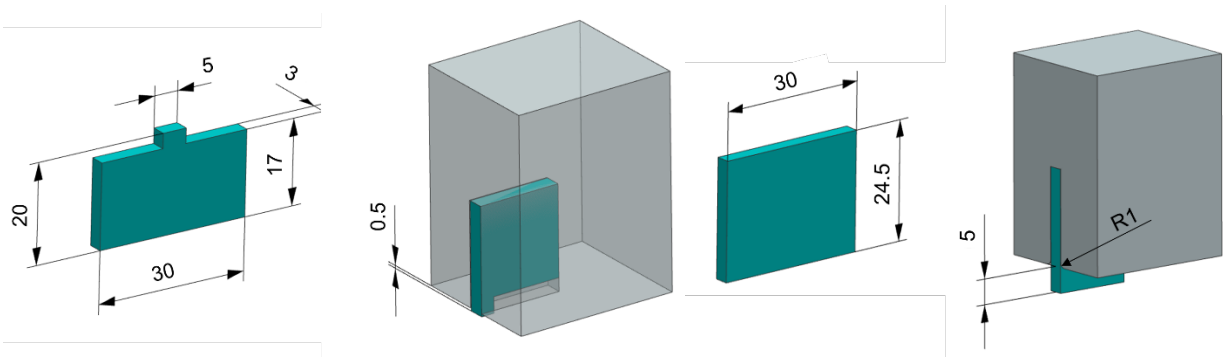

Fig. 3. Samples dimensions used in the study.

The specimens were manufactured using wire Electrical Discharge Machining (EDM), selecting cutting conditions that produced the targeted initial surface roughness. This fabrication technique was chosen because its surface texture closely resembles that obtained through Electro Discharge Texturing (EDT), which is relevant for studying how the surface roughness evolves both under straining and in cases without straining caused by surface expansion. Surface roughness characterization was performed on three independent samples using a Sensofar S-NEOX non-contact 3D optical profiler operating in interferometry mode. The measurements confirmed that the resulting surface conditions were highly consistent among the samples. The arithmetical mean height (Sa) averaged 6.62 µm with a standard deviation of 0.77 µm; the developed interfacial area ratio (Sdr) was 51.47% with a standard deviation of 6.53%; and the dale void volume at p = 80% (Vvv) reached 0.862 with a standard deviation of 0.084. A representative example of the initial surface topography is presented in Fig. 4 left.

Tooling and lubricant. The counterpart material used in this study was the 1.2379 tool steel. After milling the steel to the specified plate dimensions, it was quenched and tempered to achieve a final hardness of 60 HRc. Prior to testing, both sides of the plate were grinded to ensure the required flatness and to obtain the desired surface finish. The grinding was performed parallel to the sliding direction to facilitate optimal material flow.

Surface finish measurements, conducted using the same non-contact 3D optical profiler as the one used for the sheets, are presented in Fig. 4 right. To assess the homogeneity of the surface finish, three measurements were taken at different locations on the tool. The arithmetical mean height (Sa) was found to be 0.15 µm with a standard deviation of 0.01 µm, the developed interfacial area ratio (Sdr) was 0.35% with a standard deviation of 0.01%, and the dale void volume at p=80% (Vvv) was 0.03 with a standard deviation of 0.001

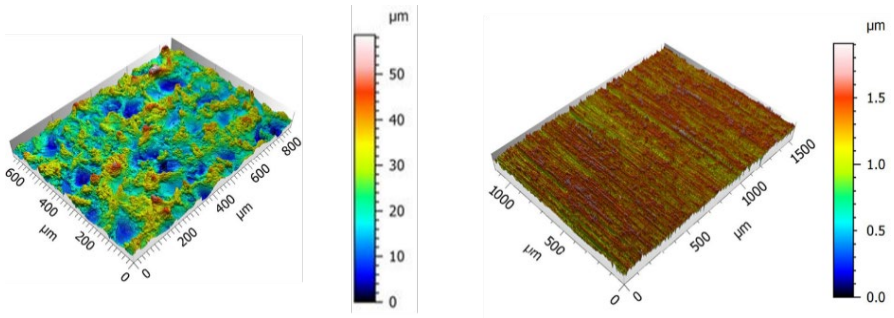

Fig. 4. Sample (left) and tool (right) roughness

The lubricant utilized in the experiments was Renoform 5200/100, provided by Fuchs. This lubricant is specifically formulated for high contact pressure applications, including fine blanking and other demanding forming processes. It possesses a kinematic viscosity of 110 cSt (mm²/s). To ensure complete saturation of oil pockets prior to testing, the tests were conducted under lubricated conditions with an excess of lubricant.

Testing conditions. Friction tests using the 5x3 mm^2 sample (nearly with no surface expansion) and the 30x3 mm2 sample (significant surface expansion) were performed using different contact pressures. Expansion of the contact surface was observed at contact pressures bigger than 100 MPa (approximately yield limit of material). The expanded surface of the 5x3 mm^2 sample for 200 MPa nominal contact pressure and the 30x3 mm^2 sample for 2.5 and 5.0 tons of force are shown in Fig. 5.

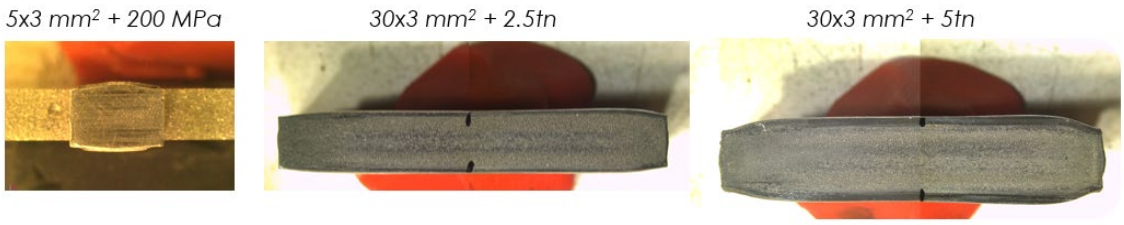

Fig. 5. Expanded contact surface for the different samples and applied forces.

When the 5x3 mm^2 sample was tested, the normal force corresponding to nominal contact pressures of 5, 10, 15, 20, 25, 50, 100, 200 MPa was applied prior to sliding. After the tests, the mean friction coefficient was obtained as explained in chapter Test description. The mean contact pressure of the test was calculated similarly using Eq. 3.

$$\bar{P} = \frac{\sum_{i=1}^{n} F_{N\_i}/n}{A} \quad (3)$$

where $\bar{P}$ is the mean contact pressure, F_{N_i} is the instantaneous normal force, n is the total amount of measured points in the evaluation area and A is the real contact area that was measured after every test using a Leica optical macroscope.

In contrast, a different methodology was employed when testing the 30x3 mm² sample. Initially, the sample was compressed using two different normal forces (2.5 and 5.0 tons), and the resulting contact surface area was measured using a Leica optical macroscope. Based on the measured contact area, the testing forces were calculated to achieve normal contact pressures of 5, 10, 15, 20, 25, 50, 100, and 200 MPa on the newly formed surfaces. The testing procedure was then as follows: First, the surface was expanded using 2.5 and 5.0 ton force. Subsequently, the normal force was reduced to the value corresponding to the desired contact pressure, and once stabilized, the sliding test was conducted. Given that the actual normal force changes during the test, the mean contact pressure was calculated post-test using Eq. 3.

It is important to note that neither the 5x3 mm² sample nor the 30x3 mm² sample achieved a contact pressure of 200 MPa, as the material underwent expansion and yielding after 100 MPa.

Results

Surface topographies. Surface topographies were measured after the test using a non-contact 3D optical profiler (Sensofar S-NEOX, interferometry technique) with an objective of 20xDI. An acquisition area of 877 µm ×660 µm was set and measurements were post processed through SensoMap Premium 7 metrology software.

As illustrated in Fig. 6, the surface topography of the 5x3 mm² sample undergoes substantial changes with increasing normal pressure. Surface roughness and void volume decrease as asperities are flattened and material from the valleys is displaced upward. A notable flattening of the surface is observed between contact pressures of 100 and 200 MPa. This pronounced flattening occurs due to the expansion of the surface, which is attributed to the material reaching its yielding point, approximately 100 MPa.

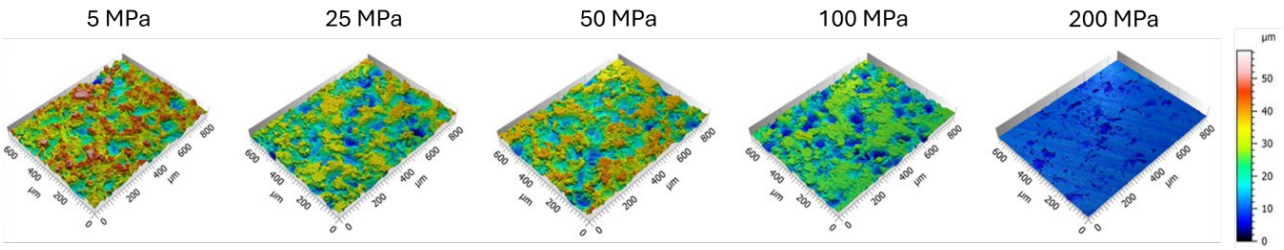

Fig. 6. Surface topographies of sample 5x3 mm2.

Fig. 7 presents the surface topographies of the 30x3 mm² sample using normal forces of 2.5 and 5.0 tons. As previously discussed, the contact surface undergoes significant expansion due to the plastic deformation of the sample, leading to substantial flattening of the initial surface roughness. This behavior is consistent with the observations made for the 5x3 mm² sample, where plastic deformation begins at approximately 100 MPa, resulting in more pronounced surface flattening beyond that caused by compression alone. Normal contact pressures shown in Fig. 7 were calculated using the equation 3.

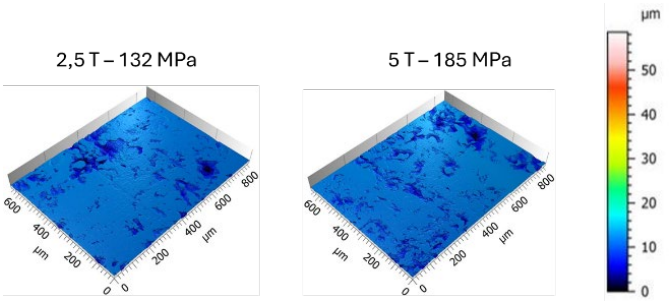

Fig. 7. Surface topographies of sample 30x3 mm2 using 2.5 and 5.0 tons of normal force.

Optical macroscope measurements confirmed that the 5x3 mm² samples exhibited expansion only after reaching a normal contact pressure of 100 MPa. A surface expansion ($SE = {}^{A_f}/_{A_0} \cdot 100$) of 133% was observed at a nominal contact pressure of 200 MPa, corresponding to a normal contact pressure of 140.7 MPa.

For the 30x3 mm² sample, a surface expansion of 187% was measured under a normal force of 2.5 tons. Further expansion was achieved with a 5.0-ton force, resulting in a surface expansion of 269%.

Friction coefficients. Mean friction coefficients for the different tested conditions and mean contact pressures are shown in Fig. 8 together with the standard deviation obtained from 3 different sheet compression sliding tests.

Results show that friction coefficient significantly depends on contact pressure and the initial surface condition (expansion ratio of the surface).

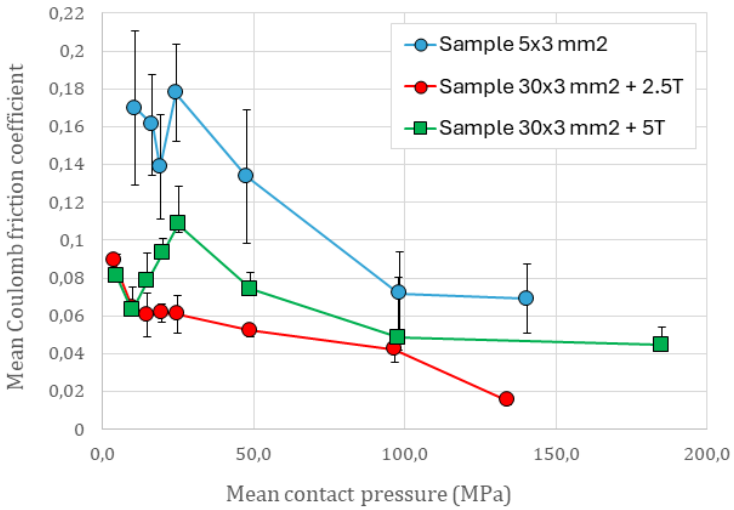

Fig. 8. Mean friction coefficients for the different conditions and mean contact pressures

Conclusions and Outlook

The newly developed Sheet Sliding Compression Test shows significant promise for the investigation of lubricants and friction conditions in cold forging and sheet metal bulk forming. The novel sample preparation methodology allows to produce various surface finishes, ranging from rough surfaces that replicate EDT (electro-discharge texturing) finishing to others such as grinding or shearing. The optimized sample designs provide control over the surface expansion of the contact area, enabling tests at different levels of surface expansion.

Friction tests conducted on an EDT-finished AA1050 aluminum sheet confirm that asperity flattening is influenced not only by normal contact pressure but also by surface expansion. This latter parameter significantly reduces surface roughness as asperities are flattened through straining, and because the combined effects of compression and expansion induce plastic deformation under complex stress conditions. This effect has been validated through surface topography measurements obtained using a confocal profilometer.

Regarding friction coefficients, it is evident that they decrease with increasing contact pressure. This phenomenon is well-documented in the literature and is attributed to the decreasing attack angle of contact patches [14] and the activation of the micro Plasto Hydrodynamic Lubrication regime under high contact pressure and sliding conditions [12].

Notably, extreme contact pressures combined with surface expansion led to significant asperity flattening and a further reduction in friction. This is particularly pronounced in friction tests conducted after a 2.5-ton compression force, which resulted in a surface expansion of 187%. In this scenario, the contact angle is likely significantly reduced, and a sufficient oil film remains on the contact surface, causing the friction coefficient to decrease to as low as 0.02. However, in tests conducted after applying a 5.0-ton force and achieving a surface expansion of 269%, friction coefficients were observed to be higher than in the previous condition. This increase in friction may be attributed to galling observed in some tests, likely due to oil being squeezed out under such high contact pressures, leaving insufficient lubricant to cover the significantly expanded surface.

Future research will involve the development of pressure and surface expansion dependent friction model using experimental data. This model will be applied to simulate a gear bulk forming process initiated from a sheet.

References

[1] Filzek, J., Ludwig, M., & Groche, P. (2011). Improved FEM simulation of sheet metal forming with friction modelling using laboratory tests. Proceedings of the IDDRG, Bilbao, Spain, 5-8.

[2] Galdos, L., Agirre, J., Mendiguren, J., Argandona, E. D., Otegi, N., & Trinidad, J. (2019). Mixed isotropic–kinematic hardening model for cold forging simulation of an industrial bolt. In Proceedings of the 52nd ICFG plenary meeting.

[3] Galdos, L., Agirre, J., Otegi, N., Mendiguren, J., & de Argandoña, E. S. (2021). Simulation of Cold Forging Processes Using a Mixed Isotropic-Kinematik Hardening Model. In Forming the Future: Proceedings of the 13th International Conference on the Technology of Plasticity (pp. 773-787). Springer International Publishing.

[4] Galdos, L., Agirre, J., Ziarsolo, U., & Atxega, M., (2023). 42CrMo4 material characterization for cold forging simulation -Comparison of different rheological laws. In Proceedings of the 53rd ICFG plenary meeting.

[5] Gil, I., Mendiguren, J., Galdos, L., Mugarra, E., & de Argandoña, E. S. (2016). Influence of the pressure dependent coefficient of friction on deep drawing springback predictions. Tribology International, 103, 266-273.

[6] Groche, P., Stahlmann, J., & Müller, C. (2013). Mechanical conditions in bulk metal forming tribometers—Part two. Tribology International, 66, 345-351.

[7] Groche, P., Kramer, P., Bay, N., Christiansen, P., Dubar, L., Hayakawa, K., ... & Moreau, P. (2018). Friction coefficients in cold forging: A global perspective. CIRP Annals, 67(1), 261-264.

[8] Hol, J., Alfaro, M. C., de Rooij, M. B., & Meinders, T. (2012). Advanced friction modeling for sheet metal forming. Wear, 286, 66-78.

[9] Hol, J., Wiebenga, J. H., & Carleer, B. (2017, September). Friction and lubrication modelling in sheet metal forming: Influence of lubrication amount, tool roughness and sheet coating on product quality, IOP Conf. In Series: Journal of Physics: Conf. Series (Vol. 896).

[10] Karupannasamy, D. K., Hol, J., de Rooij, M. B., Meinders, T., & Schipper, D. J. (2014). A friction model for loading and reloading effects in deep drawing processes. Wear, 318(1-2), 27-39.

[11] Kolpak, F., Hering, O., & Tekkaya, A. E. (2021). Consequences of large strain anisotropic work-hardening in cold forging. International Journal of Material Forming, 14, 1463-1481.

[12] Ma, X., De Rooij, M., & Schipper, D. (2010). A load dependent friction model for fully plastic contact conditions. Wear, 269(11-12), 790-796.

[13] Merklein, M., Zöller, F., & Sturm, V. (2014). Experimental and numerical investigations on frictional behaviour under consideration of varying tribological conditions. In Advanced Materials Research (Vol. 966, pp. 270-278). Trans Tech Publi-cations Ltd.

[14] Mizuno, T., & Okamoto, M. (1982). Effects of lubricant viscosity at pressure and sliding velocity on lubricating conditions in the compression-friction test on sheet metals.

[15] Sigvant, M., Pilthammar, J., Hol, J., Wiebenga, J. H., Chezan, T., Carleer, B., & van den Boogaard, A. H. (2016, No-vember). Friction and lubrication modeling in sheet metal forming simulations of a Volvo XC90 inner door. In IOP Conference Series: Materials Science and Engineering (Vol. 159, No. 1, p. 012021). IOP Publishing.

[16] Sigvant, M., Pilthammar, J., Hol, J., Wiebenga, J. H., Chezan, T., Carleer, B., & van den Boogaard, T. (2019). Friction in sheet metal forming: Influence of surface roughness and strain rate on sheet metal forming simulation results. Procedia Manufacturing, 29, 512-519.

[17] Tamai, Y., Inazumi, T., & Manabe, K. I. (2016). FE forming analysis with nonlinear friction coefficient model con-sidering contact pressure, sliding velocity and sliding length. Journal of Materials Processing Technology, 227, 161-168.

[18] Trzepiecinski, T. (2019). A study of the coefficient of friction in steel sheets forming. Metals, 9(9), 988.

[19] Wang, Z. G., Komiyama, S., Yoshikawa, Y., Suzuki, T., & Osakada, K. (2015). Evaluation of lubricants without zinc phosphate precoat in multi-stage cold forging. Cirp Annals, 64(1), 285-288.

The publication of this article was funded by the Mondragon Goi Eskola Politeknikoa, J.M.A. S.Coop